

NIKHEF 97-020  
hep-ph/9707262

## The BFKL Pomeron with running coupling constant: how much of its hard nature survives?

L.P.A. Haakman <sup>a</sup>, O.V. Kancheli <sup>b</sup>, J.H. Koch <sup>a,c</sup>

<sup>a</sup> *National Institute for Nuclear Physics and High Energy Physics (NIKHEF),  
P.O. Box 41882, NL-1009 DB Amsterdam, The Netherlands*

<sup>b</sup> *Institute of Theoretical and Experimental Physics,  
B. Cheremushinskaya 25, 117 259 Moscow, Russia*

<sup>c</sup> *Institute for Theoretical Physics, University of Amsterdam*

(7 July 1997)

We discuss the BFKL equation with a running gauge coupling and identify in its solutions the contributions originating from different transverse momentum scales. We show that for a running coupling constant the distribution of the gluons making up the BFKL Pomeron shifts to smaller transverse momenta so that the dominant part of Pomeron can have a nonperturbative origin. It is demonstrated how this soft physics enters into the BFKL solution through the boundary condition. We consider two kinematical regimes leading to different behaviour of the rapidity and transverse momentum dependence of the gluon distribution. In the diffusion approximation to the BFKL kernel with running  $\alpha_s$ , we find a sequence of poles which replaces the cut for fixed  $\alpha_s$ . The second regime corresponds to the singular part of the kernel, which gives the dominant contribution in the limit of very large transverse momenta. Finally, a simple more general picture is obtained for the QCD Pomeron in hard processes: it is of soft, nonperturbative nature, but has hard ends of DGLAP-type.

### 1. INTRODUCTION

The description of high energy reactions in terms of the exchange of a Pomeron and of secondary Reggeons continues to be very successful. Ever since the arrival of QCD, the challenge has of course been to provide an elementary, microscopic description of the Regge theory. Nonperturbative aspects have so far made it impossible to have a complete QCD description. However, in the extreme limit of very high rapidities and large transverse momenta, it was possible to model the Pomeron perturbatively by the exchange of a gluon ladder and obtain an analytic expression under certain kinematical conditions. This was called the BFKL Pomeron [1], which was considered to be of somewhat academic interest. The recent HERA experiments, which showed a very rapid increase of the structure function  $F_2(x, Q^2)$  in the limit of small  $x$ , have renewed the interest in the BFKL Pomeron, since it predicts such a behaviour. This inspired the hope that this and other features resulting from the BFKL Pomeron already start to appear at existing energies.

It is commonly assumed that the Pomeron in QCD is dominated by gluons. Due to its quantum numbers it has to consist of at least two gluons, which would result in a constant cross section as a function of energy [2]. The admixture of multigluon states and other, nonperturbative effects then should lead to the Pomeron, with glueball states on its trajectory. This trajectory should have the observed rather small

slope  $\alpha'_P$  and “supercritical” intercept  $\alpha_P(0) > 1$ . The calculations done so far, while not complete, were at least able to confirm this concept of the Pomeron.

Due to the smallness of the gauge coupling, the two gluon state is expected to dominate the Pomeron in reactions involving high transverse momenta. However, at high energies or correspondingly for high rapidities, a simple perturbative calculation of the two gluon exchange is not sufficient and interactions between the two gluons must be taken into account. This is done in the well-known BFKL Pomeron [1] in leading logarithmic approximation (LLA) in  $\log(1/x)$  with a fixed QCD coupling constant. This “hard” Pomeron can be represented by the exchanges of gluon ladders.

An interesting and characteristic feature of the BFKL Pomeron is the diffusion in the transverse momenta (in fact in the logarithms) of the gluons as the rapidity increases along the gluonic ladder. It can lead to a growth of the mean transverse momentum with energy and one expects that at very high energies the “hard Pomeron” dominates in processes with high transverse masses. In this region of high virtualities also the DGLAP evolution might be applied. For the diffusion property at fixed  $\alpha_s$  it is essential that the BFKL equation is scale invariant. Clearly it will be interesting to examine how the situation will change after this invariance is broken. Since the main source of the scale invariance violation is the dependence of the effective gauge coupling on the QCD scale  $\Lambda$ , the most obvious way to study this question is to include the running gauge coupling in the BFKL equation. Evidently there are other higher order corrections: one part concerns the BFKL gluon ladder itself [3], but one expects that they should not change its qualitative features much more; other corrections involve multiple Reggeon diagrams [4]. Some aspects of these questions have already been considered in Refs. [5–11].

It is the aim of this paper to analyse the generalization of the BFKL approach to a running coupling constant in the most straightforward fashion and to arrive at a comprehensive physical interpretation. Our numerical study in Ref. [12] of the BFKL equation with a running coupling constant has already shown that the BFKL Pomeron is of purely perturbative character only at the ends of the gluon ladder, while becoming progressively soft towards the middle. We study here the presence of a running coupling constant in more detail in an analytical fashion and, in addition, examine the singularity structure of the Pomeron in the complex angular momentum plane.

The outline of our paper is as follows. We begin with a review of the original BFKL equation with fixed coupling constant in Section 2. Then in Section 3 we present the exact solution of the BFKL equation with running  $\alpha_s$ , chosen in the simplest form for the full range of transverse momenta and without an infrared cut-off. The main result is that we find an essential singularity in the complex angular momentum plane, independent of any transverse momentum scale, that leads to an energy dependence for the cross sections of the form  $e^{c\sqrt{y}}$ . This result is further explored in the following sections. In Section 4 we examine a diffusion-like approximation to the full operator equation. We find that this diffusion solution contains an infinite sequence of poles in the complex variable  $\omega$ , the conjugate of the rapidity  $y$ . This resembles the series of poles found earlier by Lipatov [5], which replaces the cut in the case of fixed  $\alpha_s$ . We examine the residues of these poles and their importance in hard processes. A simple quantum-mechanical analogue is presented to make the essential characteristics of the diffusion solution more transparent. In Section 5, the contribution from the singular part of the BFKL kernel is discussed. It represents large increments in the transverse momenta of the gluons along the ladder and is shown to lead to a DGLAP-like behaviour. Based on the features we found for the BFKL Pomeron with running  $\alpha_s$ , we arrive at a simple more general model for the Pomeron; it reflects all the essential properties of the exact solution of Section 3. Its main point is that the Pomeron is of soft, nonperturbative origin, but can have hard ends, when probed by a hard device as in deep-inelastic scattering. In the limit of very large rapidities the hard ends become small compared to the soft part. Applications to onium-onium scattering are considered. A summary and our conclusions are contained in Section 6. The main conclusions of this paper were already reported in Ref. [13].

## 2. BFKL EQUATION WITH FIXED COUPLING CONSTANT

In this section we review shortly the BFKL equation with fixed coupling constant  $\alpha_s$ . It has been experimentally established that the hard cross sections corresponding to the exchange of vacuum quantum numbers have a power-law increase as function of the CMS energy  $\sqrt{s}$  according to  $\sigma \sim s^{\Delta_{exp}}$  with  $\Delta_{exp} \sim 0.3$ . A simple two-gluon exchange as model for the hard Pomeron [2] however leads to constant total cross sections, and diagrams leading to large  $\log(s)$  contributions must be taken into account. BFKL included such more complex diagrams which could be resummed and represented as exchanges of effective gluon ladders. In these ladders non-local gauge invariant Lipatov vertices and reggeized gluon propagators are the building blocks (see Fig.1). This was done under the assumption of “multiregge kinematics”, where the rapidity monotonically increases along the ladder in large steps,  $\delta \gg 1$ . These ladder-like configurations make the cross sections increase fast with energy. BFKL performed their calculations for fixed coupling constant  $\alpha_s$  in leading logarithmic approximation, *i.e.*

$$\alpha_s \ll 1 \quad ; \quad \alpha_s y \sim 1 \quad , \quad (2.1)$$

where the rapidity interval between the ends of the ladder,  $y$ , is related to the total energy, according to  $y \sim \log(s)$ . The simple ladder structure of the diagrams makes it possible to write a Bethe-Salpeter type of equation for this amplitude. This leads to a linear integro-differential equation, known as the BFKL equation for the low  $x$  behaviour of the unintegrated gluon distribution in the nucleon:

$$\frac{\partial f(y, k_\perp^2)}{\partial y} = \frac{3\alpha_s}{\pi} \int_0^\infty \frac{dq_\perp^2}{q_\perp^2} k_\perp^2 \left[ \frac{f(y, q_\perp^2) - f(y, k_\perp^2)}{|q_\perp^2 - k_\perp^2|} + \frac{f(y, k_\perp^2)}{\sqrt{4q_\perp^4 + k_\perp^4}} \right] \equiv \bar{\alpha}_s \mathcal{L}(k_\perp^2) \otimes f(y, k_\perp^2) \quad , \quad (2.2)$$

where we defined the rapidity as  $y = \log(x_0/x)$  with  $x_0$  a higher  $x$  value at which the initial condition should be given, and  $\bar{\alpha}_s = 3\alpha_s/\pi$ . In Eq.(2.2) the integration over the angle between  $k_\perp$  and  $q_\perp$  has already been performed. The function  $f(y, k_\perp^2)$  is proportional to the imaginary part of the virtual gluon forward scattering amplitude with vacuum quantum numbers in the  $t$ -channel; the first term of the integrand corresponds to the emission of real gluons while the second term originates from the virtual part of the amplitude. In a reaction with characteristic scale  $Q^2$ , one probes the integrated gluon distribution,

$$G(y, Q^2) = \int_{\mu^2}^{Q^2} \frac{dk_\perp^2}{k_\perp^2} f(y, k_\perp^2) \quad . \quad (2.3)$$

Since the BFKL equation is scale invariant, it can be solved in a simple way using Mellin and Laplace transformations with respect to  $k_\perp^2$  and  $y$ . Therefore we define

$$\tilde{f}(y, \beta) = \int_0^\infty \frac{dk_\perp^2}{k_\perp^2} \left( \frac{k_\perp^2}{m^2} \right)^{-\beta} f(y, k_\perp^2) = \int_{-\infty}^\infty du e^{-\beta u} f(y, u) \quad , \quad (2.4)$$

$$\bar{f}(\omega, u) = \int_0^\infty dy e^{-\omega y} f(y, u) \quad , \quad (2.5)$$

$$F(\omega, \beta) = \int_0^\infty dy e^{-\omega y} \tilde{f}(y, \beta) \quad , \quad (2.6)$$

where  $u = \log(k_\perp^2/m^2)$ , a definition we use throughout the paper, and where  $m$  is a scale introduced in order to make the transformed distribution  $\tilde{f}(y, \beta)$  in Eq.(2.4) dimensionless. The variable  $\omega$ , conjugate to the total rapidity interval  $y$ , has a physical interpretation relating it to the (complex) angular momentum:  $\omega = j - 1$ . Applying both transformations to Eq.(2.2) leads to the algebraic equation

$$\omega F(\omega, \beta) = \tilde{f}(0, \beta) + \bar{\alpha}_s \tilde{\mathcal{L}}(\beta) F(\omega, \beta) \quad , \quad (2.7)$$

with the solution

$$F(\omega, \beta) = \frac{\tilde{f}(0, \beta)}{\omega - \bar{\alpha}_s \tilde{\mathcal{L}}(\beta)} , \quad (2.8)$$

where

$$\tilde{\mathcal{L}}(\beta) = 2\Psi(1) - \Psi(\beta) - \Psi(1 - \beta) , \quad \Psi(\beta) = \frac{d \log \Gamma(\beta)}{d\beta} , \quad (2.9)$$

is the eigenvalue spectrum of the BFKL integral operator in Eq.(2.2). The Mellin transformation with respect to  $k_\perp$  was only well defined for  $0 < \text{Re } \beta < 1$ . In this range of  $\beta$  the function  $\tilde{\mathcal{L}}$  has a minimum at  $\beta = 1/2$  while it is singular at the edges  $\beta = 0$  and  $\beta = 1$  (see Fig.2). The limit  $\beta \rightarrow 0$  corresponds to the hard limit, where  $u$  is large.

We take the inverse transformations over  $\beta$  and  $\omega$  of Eq.(2.8) to get back to  $f(y, u)$

$$\tilde{f}(y, \beta) = \frac{1}{2\pi i} \int_{c-i\infty}^{c+i\infty} d\omega e^{\omega y} F(\omega, \beta) , \quad (2.10)$$

$$f(y, u) = \frac{1}{2\pi i} \int_{d-i\infty}^{d+i\infty} d\beta e^{u\beta} \tilde{f}(y, \beta) , \quad (2.11)$$

with  $c$  a real number to the right of all singularities in  $\omega$  and  $d$  an appropriately chosen real number between 0 and 1. This yields the solution of the BFKL equation

$$f(y, u) = \int_{-\infty}^{\infty} du' f(0, u') \mathcal{G}_f(y, u - u') , \quad (2.12)$$

where  $f(0, u')$  is the boundary condition at  $y = 0$ , and with the Green's function

$$\mathcal{G}_f(y, u) = \frac{1}{2\pi i} \int_{\frac{1}{2}-i\infty}^{\frac{1}{2}+i\infty} d\beta \exp\left(\beta u + y \bar{\alpha}_s \tilde{\mathcal{L}}(\beta)\right) , \quad (2.13)$$

where we took  $d = 1/2$  due to the pinch of the  $\beta$  contour at the point  $\beta = 1/2$ . This pinch results in a leading singularity in Eq.(2.8) at  $\omega = \bar{\alpha}_s \tilde{\mathcal{L}}(1/2)$ . For large  $y$  the saddle point method can be used to calculate explicitly the Green's function. With the help of the expansion of the kernel around  $\beta = 1/2$ ,

$$\bar{\alpha}_s \tilde{\mathcal{L}}(\beta) \approx \Delta + B(\beta - \frac{1}{2})^2 ; \quad \Delta = 4\bar{\alpha}_s \log(2) , \quad B = 14\bar{\alpha}_s \zeta(3) , \quad (2.14)$$

one then obtains

$$\mathcal{G}_f(y, u) \approx \frac{1}{\sqrt{4\pi B y e^{-u}}} \exp\left(y\Delta - \frac{u^2}{4By}\right) . \quad (2.15)$$

The character of the corresponding singularity in  $\omega$  and its dependence on  $u$  can be more easily seen in the  $(\omega, u)$ -representation where the Green's function takes the form

$$\mathcal{G}_f(\omega, u) \approx \frac{1}{\sqrt{4B e^{-u}(\omega - \Delta)}} \exp\left[-u\sqrt{\frac{\omega - \Delta}{B}}\right] , \quad (2.16)$$

which shows the branch point singularity at  $\omega = \Delta$ .

From Eqs.(2.12) and (2.15) we see the two characteristic features of the BFKL Pomeron. First, the Pomeron intercept  $\Delta \simeq 2.6 \alpha_s$  is relatively large, of order 0.5 for a realistic  $\alpha_s \sim 0.2$ . Therefore the observed energy dependence of cross sections by the HERA experiments,  $\sigma \sim s^{\Delta_{exp}}$ , was seen as a possible sign of the appearance of the BFKL Pomeron in hard scatterings. Second, the diffusion of the  $u$  distribution as  $y$  grows:  $\langle (u - \bar{u})^2 \rangle \sim 4By$ . As will be seen later, this important diffusion property is a consequence of scale invariance when  $\alpha_s$  is fixed.

We conclude this section with two comments about the applicability of the BFKL Pomeron in LLA. Due to the diffusion of the  $u$  distribution, it can happen that as  $y \rightarrow \infty$  one reaches regions of small transverse momenta, where non-perturbative effects take place. For the perturbative BFKL Pomeron to be applicable, these contributions should be small. One can simply exclude transverse momenta below some fixed  $k_{\perp}^{min}$  in all gluon ladder diagrams by introducing a cut-off in the integral that enters into the BFKL equation [14,15]. Another way to achieve this is to consider the BFKL Pomeron in onium-onium scattering. In this case there is a purely perturbative regime near both ends of the gluon chain due to the small transverse sizes of the onia,  $R_{\perp}^2 \sim 1/k_{\perp}^2$ . They can be chosen sufficiently small, so that the transverse momenta in the gluon ladder do not reach the infrared region in the entire rapidity interval between the two onia. In the numerical examples in Ref. [12], the influence of the small  $k_{\perp}^2$  region on the gluon ladder was found to be not large for fixed  $\alpha_s$ ; the gluons in the ladder are in the mean far from the soft region. However, for running  $\alpha_s$  the diffusion to the infrared region was shown to proceed much faster.

Concerning the assumption of multiregge kinematics, we can make the following estimate for the BFKL Pomeron, based on a general property, independent from the underlying QCD dynamics. For a ladder diagram with vector particle exchange the cross section grows as  $e^{y\Delta}$ . Expanding this exponential function as  $\sum_n (y\Delta)^n / n!$ , one obtains the cross section in terms of contributions from ladders with  $n$  rungs and a corresponding mean multiplicity  $\bar{n} = y\Delta$ . As result, the mean rapidity interval between neighbouring rungs is  $\bar{\delta} \equiv \langle y_i - y_{i+1} \rangle \simeq \Delta^{-1}$ . This quantity is not large: for  $\alpha_s \simeq 0.2$  one has  $\bar{\delta} \sim 2$  or  $\Delta \simeq 0.5$ . However, the BFKL was derived under the assumption of multiregge kinematics,  $\bar{\delta} \gg 1$ . If we consider ladders making up the Pomeron with a lower cut-off,  $\delta_0 \simeq 1$ , for the rapidity difference  $\delta = y_i - y_{i+1}$ , a sizeable fraction of the gluons are eliminated. This is due to the fact that the gluons are concentrated at small rapidity differences as was confirmed numerically in Ref. [12]. For  $\alpha_s = 0.2$  it was found that the new  $\Delta$  characterizing the resulting energy dependence of the cross section becomes smaller by approximately a factor of two.

### 3. EXACT SOLUTIONS OF BFKL WITH RUNNING $\alpha_s$

In this section we include a running coupling constant in the BFKL equation. The procedure to do this is not unique. It is often required that the so-called ‘‘bootstrap condition’’ [5] is obeyed. This consistency condition follows from the requirement that the solution of the BFKL equation in the gluon colour octet channel should be that of the reggeized gluon itself. Further one should check that in the limit of very high transverse momenta the double logarithmic approximation of the DGLAP equation is obtained. Nevertheless, many ways to introduce a running gauge coupling  $\alpha_s$  in the BFKL equation remain possible, but they are expected only to result in non-essential corrections.

We include a running coupling constant in the BFKL equation by using instead of the fixed one in Eq.(2.2) the perturbative expression

$$\alpha_s(k_{\perp}^2) = \frac{1}{b \log(k_{\perp}^2/\Lambda^2)} , \quad (3.1)$$

where  $\Lambda$  is the QCD scale parameter and  $b = (33 - 2N_f)/12\pi$ . This choice was also made in Ref. [5,9]. We put the running coupling constant under the integral in the following way:

$$\frac{\partial f(y, k_{\perp}^2)}{\partial y} = \frac{3}{\pi} \int_0^{\infty} \frac{dq_{\perp}^2}{q_{\perp}^2} k_{\perp}^2 \left[ \frac{\alpha_s(q_{\perp}^2) f(y, q_{\perp}^2) - \alpha_s(k_{\perp}^2) f(y, k_{\perp}^2)}{|q_{\perp}^2 - k_{\perp}^2|} + \frac{\alpha_s(k_{\perp}^2) f(y, k_{\perp}^2)}{\sqrt{4q_{\perp}^4 + k_{\perp}^4}} \right] . \quad (3.2)$$

This has precisely the structure of the original BFKL equation when we write  $h(y, k_\perp^2) = \alpha_s(k_\perp^2) f(y, k_\perp^2)$ :

$$\frac{\partial h(y, k_\perp^2)}{\partial y} = \alpha_s(k_\perp^2) \mathcal{L}(k_\perp^2) \otimes h(y, k_\perp^2) . \quad (3.3)$$

It is also possible to leave the running coupling constant  $\alpha_s(k_\perp^2)$  outside the integral. In this case we obtain a modified BFKL equation as in Eq.(3.3), but now for  $f(y, k_\perp^2)$  instead of  $h(y, k_\perp^2)$ . Therefore it yields a gluon distribution with an additional factor  $\alpha_s(k_\perp^2)$  as compared to our choice where it is put under the integral. As we will see later, our method is the one that leads to the correct behaviour for large transverse momenta.

We begin with a qualitative argument in order to show how including a running  $\alpha_s$  in the BFKL equation can modify the characteristic BFKL features. For constant  $\alpha_s$  the large rapidity behaviour of the total cross section predicted by the BFKL equation is given by  $\sigma(y) \sim \exp(y\alpha_s 12 \log(2)/\pi)$ . The  $\alpha_s$  entering this expression should be taken at some fixed, effective value of  $k_\perp$  that must be of the order of the mean  $k_\perp$  in the gluonic ladder representing the Pomeron. However, for moderate transverse momenta at the lower end of the gluon ladder and a high virtuality at the top of the ladder (*e.g.* in deep inelastic scattering), the mean  $\log(k_\perp^2)$  changes along the ladder and is proportional to  $\sqrt{y}$ . Therefore, a simple estimate for the effect of a running coupling constant can be obtained by using  $\alpha_s \sim 1/\sqrt{y}$ , leading to a cross section  $\sigma(y) \sim e^{c\sqrt{y}}$ . This behaviour is also what we find in the double logarithmic approximation of the DGLAP equation. As we will see later, in the complex angular momentum plane  $\omega = j - 1$  it corresponds to an essential singularity of  $\exp(1/\omega)$  type.

By using  $\alpha_s$ , Eq.(3.1), for all  $k_\perp$  we partly suppress the infrared region, which is in line with our goal to investigate the influence of a running  $\alpha_s$  on the structure of the BFKL Pomeron at large  $k_\perp$ . Qualitatively this may be understood from the fact that the contribution of a ladder for vector exchange, with  $n$  rungs and in a limited region of integration over  $k_\perp$ , results in amplitudes of the form

$$[\alpha_s(\bar{\mu}^2) \mathcal{D}]^n \frac{y^n}{n!} , \text{ with } \alpha_s(\bar{\mu}^2) \mathcal{D}(\mu_1, \mu_2) = \int_{k_\perp^2 > \mu_1^2}^{k_\perp^2 < \mu_2^2} d^2 k_\perp \alpha_s(k_\perp^2) [...] \quad (\mathcal{D} > 0) , \quad (3.4)$$

where  $\bar{\mu}$  the mean scale at which the running coupling constant has to be taken. In this way one obtains a Pomeron intercept with  $\Delta_0 \sim \alpha_s(\bar{\mu}^2) \mathcal{D}$ . Hence we see that the simplest way to suppress the soft contribution is to make  $\alpha_s$  negative for small  $k_\perp$  so that the corresponding singularity moves to the left half  $\omega$ -plane. Therefore it is not bad that the standard expression for  $\alpha_s$ , Eq.(3.1), has this property for  $k_\perp^2 < \Lambda^2$ . Note also that the singularity in Eq.(3.1) is integrable at  $k_\perp^2 = \Lambda^2$ .

As in the case of constant  $\alpha_s$ , we solve the BFKL equation with running  $\alpha_s$ , Eq.(3.3), by using the Laplace and Mellin transformations of Eqs.(2.4) and (2.6). In the Mellin transformation of Eq.(2.4) we set  $m^2 = \Lambda^2$ . With the help of the simple identity

$$\left(\frac{k_\perp^2}{\Lambda^2}\right)^{-\beta} \log\left(\frac{k_\perp^2}{\Lambda^2}\right) = -\frac{\partial}{\partial \beta} \left(\frac{k_\perp^2}{\Lambda^2}\right)^{-\beta} , \quad (3.5)$$

we then obtain for the Mellin transformed differential equation for the distribution  $h(y, u)$

$$-\frac{\partial^2 \tilde{h}(y, \beta)}{\partial y \partial \beta} = \tilde{\alpha}_s \tilde{\mathcal{L}}(\beta) \tilde{h}(y, \beta) , \quad (3.6)$$

where  $\tilde{\mathcal{L}}(\beta)$  is the standard BFKL kernel, Eq.(2.9), and we denoted  $\tilde{\alpha}_s = 3/\pi b$ . Further we perform the Laplace transform over the rapidity  $y$  which yields for Eq.(3.6)

$$\frac{\partial H(\omega, \beta)}{\partial \beta} = \frac{1}{\omega} \left\{ H_0(\beta) - \tilde{\alpha}_s \tilde{\mathcal{L}}(\beta) H(\omega, \beta) \right\} , \quad (3.7)$$

with  $H_0(\beta)$  a function determined from the initial condition at  $y = 0$ ,

$$H_0(\beta) = \frac{\partial \tilde{h}(0, \beta)}{\partial \beta} . \quad (3.8)$$

The homogeneous solution of Eq.(3.7) is

$$H_H(\omega, \beta) = H_H(\omega, \beta_0) \exp \left[ -\frac{\tilde{\alpha}_s}{\omega} (\mathcal{R}(\beta) - \mathcal{R}(\beta_0)) \right] , \quad (3.9)$$

where

$$\mathcal{R}(\beta) = \int^{\beta} d\beta' \tilde{\mathcal{L}}(\beta') = 2\Psi(1)\beta - \log \left[ \frac{\Gamma(\beta)}{\Gamma(1-\beta)} \right] . \quad (3.10)$$

The function  $\mathcal{R}(\beta)$  is plotted in Fig.2. Thus the total solution becomes

$$H(\omega, \beta) = H_H(\omega, \beta) + \frac{1}{\omega} \int_{\beta_0}^{\beta} d\beta' H_0(\beta') \frac{H_H(\omega, \beta')}{H_H(\omega, \beta')} . \quad (3.11)$$

This is the exact solution of the BFKL equation with a running coupling constant.

It is essential that Eq.(3.11) has only a fixed singularity at  $\omega = 0$ , *i.e.* not depending on  $\beta$ . This is in contrast to the situation with a fixed  $\alpha_s$  where the analogous solution in the  $(\omega, \beta)$ -representation is given in Eq.(2.8), and results in a  $\beta$  dependent  $\omega$ -pole. For running  $\alpha_s$  there are no pinch and endpoint singularities when carrying out the inverse tranformations needed to obtain the solution as function of  $y$  and  $u$ , since also the singularities in  $\beta$  are not dependent on  $\omega$ .

For the purpose of studying the  $y$  dependence or, equivalently, the  $\omega$  structure, we want to focus on the first term in Eq.(3.11). The second term does not introduce any new singularities in  $\omega$  since its integrand is proportional to the first term and singularities in  $\omega$  are independent of  $\beta$ . The solution of the BFKL equation with running coupling constant then becomes in the  $(\omega, u)$ -representation

$$\bar{h}(\omega, u) = \bar{h}(\omega, u_0) \frac{\bar{K}_r(\omega, u)}{\bar{K}_r(\omega, u_0)} , \quad (3.12)$$

with  $\bar{K}_r(\omega, u)$  given by

$$\bar{K}_r(\omega, u) = \frac{1}{2\pi i} \int_{d-i\infty}^{d+i\infty} d\beta \exp \left[ \beta u - \frac{\tilde{\alpha}_s}{\omega} \mathcal{R}(\beta) \right] . \quad (3.13)$$

The function  $\bar{h}(\omega, u_0)$  is determined by the boundary condition for  $u$  at  $u_0$ . The function  $h(y, u)$ , which will yield the gluon distribution as function of rapidity and transverse momentum, can finally be obtained from the inverse Mellin transformation of Eq.(3.12) with respect to  $\omega$ .

We now discuss an explicit solution of the BFKL equation with running coupling constant at very hard scales, appropriate for deep inelastic scattering. In this case we expect to find the double logarithmic approximation in  $\log(1/x)$  and  $\log(k_\perp^2)$  of DGLAP. The large transverse momentum behaviour is determined by the low  $\beta$  limit of Eq.(3.13). We can then use

$$[\Gamma(\beta)]^{\tilde{\alpha}_s/\omega} \simeq \beta^{-\tilde{\alpha}_s/\omega} , \quad (3.14)$$

and the inverse Mellin transformation in Eq.(3.13) can be easily evaluated. Only the singularity at  $\beta \sim 0$  is important; contributions to  $\bar{h}(\omega, u)$  from cuts starting at  $\beta = -1, -2, \dots$  have additional factors  $e^{-u}$ ,  $e^{-2u}, \dots$  and thus can be neglected at large  $u$ . After deformation of the path along the imaginary axis we can use Hankel's contour integral formula for  $\Gamma$ -functions [17] and obtain

$$\bar{h}(\omega, u) \simeq \frac{\bar{h}(\omega, u_0)}{\bar{K}_r(\omega, u_0)} \frac{1}{2\pi i} \int_C d\beta e^{u\beta + 2\Psi(1)\beta\tilde{\alpha}_s/\omega} \left(\frac{1}{\beta}\right)^{\tilde{\alpha}_s/\omega} \simeq \frac{\bar{h}(\omega, u_0)}{\bar{K}_r(\omega, u_0)} \frac{1}{\Gamma(\tilde{\alpha}_s/\omega)} u^{-1+\tilde{\alpha}_s/\omega} . \quad (3.15)$$

The interpretation of this solution is more transparent if we rewrite it in the more familiar form

$$\bar{f}(\omega, u) = \frac{1}{\alpha_s(u)} \bar{h}(\omega, u) \sim \bar{f}(\omega, u_0) \left[ \frac{1}{\alpha_s(u)} \right]^{\frac{1}{2\pi b}\gamma_{gg}(\omega)} \quad \text{with} \quad \gamma_{gg}(\omega) = \frac{6}{\omega} . \quad (3.16)$$

In this form for  $\bar{f}(\omega, u)$ , we recognize the anomalous dimension  $\gamma_{gg}(\omega)$ , thus showing that we indeed arrive in this limit at the DGLAP solution. As was remarked earlier, we could have placed the running coupling constant outside the integral in the BFKL equation. We would then have obtained as a result of that equation directly the function  $\bar{f}(\omega, u)$ , the gluon distribution. In that case the gluon distribution differs by an extra factor  $\alpha_s(u) \sim 1/u$ , yielding a discrepancy from DGLAP.

An important ingredient in the solutions is the boundary condition at low transverse momenta  $\bar{f}(\omega, u_0)$  which provides the function  $\bar{h}(\omega, u_0)$  in Eq.(3.12). Poles in  $\bar{f}(\omega, u_0)$  at  $\omega = \Delta_i$  result in a rapidity dependence  $e^{\Delta_i y}$ . A choice for the boundary condition is that there are no poles in the right half plane and thus no supercritical contribution originating from the region of small  $u$ . The singularities of  $\bar{f}(\omega, u_0)$  are now to the left of  $\omega = 0$  and thus not important, and the hard part of the Pomeron dominates. In that case the dominant part in the limit  $\beta \sim 0$  is contained in the function  $\bar{K}_r(\omega, u)$  of Eq.(3.13). Such an approach which is only based on the  $\bar{K}_r(\omega, u)$  and not on boundary conditions could in the past provide a reasonable description of the first HERA data. The present low  $x$  data show the need of a supercritical intercept input. The Mellin transformation from  $\omega$  to  $y$  can be performed and yields a modified Bessel function  $I_1$ . Thus one finds for  $\bar{K}_r(y, u)$  after inverse transformations over  $\omega$  and  $\beta$

$$K_r(y, u) = \frac{1}{2\pi i} \int_{d-i\infty}^{d+i\infty} d\beta e^{u\beta} \sqrt{\left(\frac{\tilde{\alpha}_s \mathcal{R}(\beta)}{y}\right)} I_1(2\sqrt{y\tilde{\alpha}_s \mathcal{R}(\beta)}) . \quad (3.17)$$

For large rapidities one may use  $I_1(y) \simeq e^y / \sqrt{2\pi y}$  so that Eq.(3.17) simplifies to

$$K_r(y, u) = \frac{1}{2\pi i} \int_{d-i\infty}^{d+i\infty} d\beta \left(\frac{\tilde{\alpha}_s \mathcal{R}(\beta)}{16\pi^2 y^3}\right)^{1/4} \exp\left(u\beta + 2\sqrt{y\tilde{\alpha}_s \mathcal{R}(\beta)}\right) . \quad (3.18)$$

By using the method of steepest descent, the inverse Mellin transformation then yields the standard double logarithmic approximation to the DGLAP equation

$$K_r(y, u) \sim u^{-1} \left(\frac{\tilde{\alpha}_s \log u}{16\pi^2 y^3}\right)^{1/4} \exp\left(\sqrt{4\tilde{\alpha}_s y \log u}\right) . \quad (3.19)$$

This solution corresponds to the well known double logarithmic approximation where not only a strong monotonous increase of rapidity is imposed, but also a strong ordering of the transverse momenta along the ladder. It thus means that the resulting cross section grows as  $e^{c\sqrt{y}}$ , slower than for the observed “supercritical Pomeron”, which behaves as  $e^{y\Delta_{exp}}$ .

The above boundary condition seems not to be realistic if one tries to describe the soft high energy processes, by assuming the existence of only one Pomeron, containing both soft and hard mechanisms. In the case where we expect the existence of a supercritical Pomeron ( $\alpha_P(0) = 1 + \Delta_0 > 1$ ) coming from QCD interactions in the nonperturbative region, we can choose as boundary condition

$$\bar{f}(\omega, u_0) = \frac{\bar{f}_0}{\omega - \Delta_0} . \quad (3.20)$$

Since  $\Delta_0 > 0$  is to the right of the essential singularity of  $\bar{K}_r(\omega, u)$ , the boundary condition gives the dominant contribution at large  $y$  while the singularity of  $\bar{K}_r(\omega, u)$  at  $\omega = 0$  represents the hard corrections. (Strictly speaking, at the boundary  $u = u_0$  the behaviour of the gluon density may have to be chosen also in accordance with the BFKL equation because, depending on  $u_0$ , the perturbative dynamics contained in the BFKL equation may already apply.) To analyse the influence of the soft, low transverse momentum region in the BFKL equation one can introduce a lower cut-off in the integrals over  $k_\perp$  in the BFKL equation. But it is more complicated to apply this method to the case of a running  $\alpha_s$  than for a fixed one [14,15]. In the next sections, we will discuss in more detail the physical picture of the gluon ladder for this choice of boundary condition corresponding to supercritical behaviour. If one supplies the boundary condition (3.20) the mean transverse momenta in inelastic processes will not grow with energy; this will also be seen later.

The main result of this section is that the hard part of the BFKL Pomeron for the case of a running  $\alpha_s$  leads to a cross section behaving as  $e^{c\sqrt{y}}$ , growing slower with  $y$  than the usual “supercritical” Pomeron. The situation where the leading  $y$  dependence is found to be determined through the boundary condition, rather than the BFKL kernel, will be discussed below.

#### 4. THE DIFFUSION APPROXIMATION TO THE BFKL KERNEL WITH RUNNING $\alpha_s$

We now discuss two main aspects which determine the character of a parton cascade represented by our effective gluon ladders. They are the branching of the gluons leading to an exponential growth of their number with rapidity and the gluon diffusion in the transverse momentum plane. Both determine how the cascade evolves from the fragmentation region of a fast particle towards “wee” partons. Of particular importance is whether the branching and diffusion velocities depend on  $k_\perp$ . In asymptotically free theories the branching velocity becomes small for high  $k_\perp$ . In this case all properties of the parton distribution at large  $k_\perp$  will be determined by the relative weight of the diffusion and the DGLAP-evolution of partons towards larger  $k_\perp$ . The scale invariant BFKL equation with *fixed*  $\alpha_s$  has the unique property that the splitting probabilities of partons do not depend on  $k_\perp$ . Therefore the distribution of partons in  $k_\perp$  will be determined entirely by the initial distribution at the end of the ladder, which for large  $y$  is spread out over an increasingly larger interval of  $k_\perp$  by the diffusion mechanism. In this section we will study these two aspects for the BFKL Pomeron for running  $\alpha_s$ .

##### A. The diffusion-like part in the operator equation

Due to its convolution structure, it is possible to rewrite the BFKL equation Eq.(3.3) as

$$\frac{1}{\alpha_s(u)} \frac{\partial h(y, u)}{\partial y} = \frac{3}{\pi} \mathcal{L}(\hat{\beta}) h(y, u) . \quad (4.1)$$

Here  $\hat{\beta}$  is an operator acting in the space of functions depending on  $u$ . It follows from the form of the Mellin transformation that the operator is conjugated to  $u$ :  $\hat{\beta} = \frac{\partial}{\partial u}$ . A useful property of the operator kernel  $\mathcal{L}$  is that it satisfies the “shifting relation”

$$e^{cu} \mathcal{L}(\hat{\beta} + c) e^{-cu} = \mathcal{L}(\hat{\beta}) , \quad (4.2)$$

which can be proven by showing that both sides have identical Mellin transforms,  $\tilde{\mathcal{L}}(\beta)$ . As a consequence the “shifted” functions  $h_c(y, u) = e^{cu/2} h(y, u)$  obey the differential equation

$$\frac{1}{\alpha_s(u)} \frac{\partial h_c(y, u)}{\partial y} = \frac{3}{\pi} \mathcal{L}(\hat{\beta} + c/2) h_c(y, u) . \quad (4.3)$$

Because we know the dependence of the BFKL integral operator on the variable  $\beta$  through  $\tilde{\mathcal{L}}$  given by Eq.(2.9), it is possible to find a diffusion approximation. The function  $\tilde{\mathcal{L}}(\beta)$  has a minimum at  $\beta = 1/2$  as can be seen from Eq.(2.14). For Eq.(4.3) it means that the first order derivative with respect to  $u$  vanishes when the argument of  $\mathcal{L}$  equals 1/2. We therefore choose  $c = 1$  in Eq.(4.3) and expand in  $\hat{\beta}$ . We introduce the function  $h_1(y, u) = e^{-u/2} h(y, u)$  and neglect third and higher order derivatives, which leads to the differential equation

$$\frac{1}{b\alpha_s(u)} \frac{\partial h_1}{\partial y} \simeq \tilde{\Delta} h_1 + \tilde{B} \frac{\partial^2 h_1}{\partial u^2} \quad ; \quad \tilde{\Delta} = 4\tilde{\alpha}_s \log(2) , \quad \tilde{B} = 14\tilde{\alpha}_s \zeta(3) . \quad (4.4)$$

This equation resembles a diffusion equation with branching, but with a diffusion coefficient  $\alpha_s(u)b\tilde{B}$  and a branching coefficient  $\alpha_s(u)b\tilde{\Delta}$ . Here the rapidity  $y$  plays the role of time and  $u$  that of place. This analogy will be useful for understanding the structure of the function  $h(y, u)$ . The diffusion coefficient can be interpreted as a diffusion velocity, determining how fast the gluons diffuse in  $y$ . Since it is proportional to  $\alpha_s(u)$ , the gluons diffuse slowly to large  $u$ ; the region  $\beta \sim 1/2$  corresponds to an evolution where changes of  $u$  in individual steps are not large. Eq.(4.4) must be supplemented with some boundary conditions at small  $u = u_0$ , representing infrared low  $k_\perp$  physics not contained in Eq.(4.4).

For the case with fixed  $\alpha_s$ , Eq.(4.4) is a standard diffusion equation with branching,

$$\frac{\partial h_1}{\partial y} = \Delta h_1 + B \frac{\partial^2 h_1}{\partial u^2} , \quad (4.5)$$

where the branching and diffusion coefficient are independent of  $u$ . The solution  $h(y, u) = e^{u/2} h_1(y, u)$  is then given by Eq.(2.12) with the Green's function (2.13). It should therefore be clear from Eq.(4.5) that for the diffusion behaviour predicted by BFKL scale invariance is essential.

We have seen above that the region  $\beta \sim 1/2$  corresponds to an evolution where changes of  $u$  in individual steps are not large:  $\delta u \sim \alpha_s$ . On the other hand, large jumps in  $u$  are related to the region  $\beta \sim 1/u \rightarrow 0$ , where  $\tilde{\mathcal{L}}(\beta) \sim 1/\beta$  and for which  $\delta u \sim \alpha_s u$ . In this case we have to set  $c = 0$  and expand around  $\beta = 0$ ; this will be done in the next section.

With our choice for  $\alpha_s(u)$ , Eq.(3.1), the differential equation (4.4) becomes

$$u \frac{\partial h_1}{\partial y} = \tilde{\Delta} h_1 + \tilde{B} \frac{\partial^2 h_1}{\partial u^2} . \quad (4.6)$$

A solution of Eq.(4.6) can be simply found by performing a Laplace transformation with respect to  $y$ . For the transformed function  $\bar{h}(\omega, u)$  it follows that it satisfies the differential equation

$$u \omega \bar{h}(\omega, u) = \tilde{\Delta} \bar{h}(\omega, u) + \tilde{B} \frac{\partial^2 \bar{h}(\omega, u)}{\partial u^2} , \quad (4.7)$$

where for simplicity and without loss of generality for the present discussion we took  $h(0, u) = 0$ . By using the substitution  $u = z(\tilde{B}/\omega)^{1/3} + \tilde{\Delta}/\omega$  the differential equation (4.7) transforms into the Airy equation,  $f''(z) - zf(z) = 0$ , which has the solution

$$\bar{h}(\omega, u) = \text{Ai}(z) ; \quad z = \left( \frac{\omega}{\tilde{B}} \right)^{1/3} \left( u - \frac{\tilde{\Delta}}{\omega} \right) , \quad (4.8)$$

where  $\text{Ai}$  is the Airy function that is finite at  $z \rightarrow \infty$ . We note that  $\text{Ai}$  is related to the modified Bessel function  $K_{1/3}$  through  $\text{Ai}(z) = (1/\pi)\sqrt{(z/3)}K_{1/3}(2z^{2/3}/3)$ .

Before we give a full analysis of the solution (4.8) in the next section, we first examine the dominant behaviour at large  $u$ . If we assume a boundary condition for  $h_1(y, u)$  at small  $u$  of the form

$$h_1(y, u_0 \sim 1) \sim f_0 e^{\Delta_0 y} , \quad (4.9)$$

then for  $u \gg 1$  one can try to find a solution of Eq.(4.6) in the form

$$h_1(y, u) \sim \exp(\Delta_0 y - C_0 u^s - C_1 u^{s-1} - \dots) . \quad (4.10)$$

Upon inserting Eq.(4.10) into Eq.(4.6) and comparing the leading terms in  $u$  which are proportional to  $u h_1(y, u)$ , we find that  $s = 3/2$  and  $\Delta = \tilde{B} C_0^2 s^2$ . Furthermore, comparison of terms proportional to  $h_1(y, u)$  gives  $\tilde{\Delta} = 2s(1-s)\tilde{B}C_0C_1$ . Solving for  $C_0$  and  $C_1$  results in

$$s = 3/2 , \quad C_0 = \pm \frac{2}{3} \left( \frac{\Delta_0}{\tilde{B}} \right)^{1/2} , \quad C_1 = \mp \frac{\tilde{\Delta}}{\tilde{B}} \left( \frac{\Delta_0}{\tilde{B}} \right)^{-1/2} . \quad (4.11)$$

We have two solutions, positive and negative. Because a fast increase in  $u$  must be rejected, only the positive solution is accepted for  $C_0$ <sup>1</sup>. An important point is that the hard Pomeron disappears in the case of running  $\alpha_s$  in this approximation, because the residue belonging to the pole at  $\omega = \Delta_0$  rapidly decreases proportional to  $\exp(-C_0 u^{3/2})$  on a scale  $u \sim C_0^{-2/3} \sim 1$ . (The scale for the disappearance of this solution is set by  $\Delta_0$ ; the closer it is to the critical value  $\Delta_0 = 0$ , the longer the hard part of the Pomeron survives.) A significant large  $u$  contribution can therefore only come from the region  $\beta \rightarrow 0$  in  $\tilde{\mathcal{L}}(\beta)$ , which will be discussed later.

The result (4.10) can be explained in a simple fashion that shows how the transverse momentum in the gluon cascade evolves as function of rapidity  $y$  in the limit  $u \gg 1$ . Assume that starting from the soft (*i.e.* small  $u$ ) end of the gluon ladder the gluons are in the strong coupling region up to rapidities  $y - y_1$ ; in this region the gluon distribution should then be proportional to  $h_{\text{soft}}(y - y_1, u) \sim e^{\Delta_0(y-y_1)}$ . After that, in the remaining part of the rapidity interval  $y_1$ , the gluons reach large virtualities  $u$  on the other end through the diffusion-like mechanism. This last stage is described by the solution of Eq.(4.6), which for large  $u$  becomes

$$h_{\text{hard}}(y, u) \sim \exp(\tilde{\Delta}y/u - u^3/9\tilde{B}y) . \quad (4.12)$$

Using this function, we can obtain the gluon distribution for the full  $y$  range through the integral

$$h_1(y, u) \sim \int_0^y dy_1 e^{\Delta_0(y-y_1)} h_{\text{hard}}(y_1, u) . \quad (4.13)$$

This integral can be estimated at large  $y$  by the saddle point method which gives

$$h_1(y, u) \sim \exp \left[ \Delta_0 y - u^{3/2} \frac{2}{3} \left( \frac{\Delta_0}{\tilde{B}} \right)^{1/2} \right] , \quad (4.14)$$

---

<sup>1</sup>It is interesting that if QCD was not asymptotically free (for example due to a large number of fermions), then the diffusion in  $u$  described by Eq.(4.6) would go in the opposite direction of large  $u$ . In such a situation only the theory with a fixed limit makes sense when  $\alpha_s(u) \rightarrow \alpha_{\text{max}}$  for  $u \rightarrow \infty$ . So in this case the diffusion in  $u$  will move gluons in the gluonic ladder to higher  $u$  and thus the Pomeron will develop according to the BFKL solution (2.12) with constant  $\alpha_s = \alpha_{\text{max}}$ .

coinciding with the main term in Eq.(4.10). In Eq.(4.13) the mean  $y_1$  is of the order

$$\langle y_1 \rangle \sim u^{3/2} \frac{1}{3\sqrt{\tilde{B}\Delta_0}} . \quad (4.15)$$

This shows that at large  $y$  the hard part of the Pomeron is concentrated on its end. But these statements about the structure of the end part of the gluon ladder given by the expressions Eq.(4.10) and Eq.(4.15) do not concern the dominant term, since its residue is very small.

### B. The infinite sequence of poles

In this subsection we further study the solution (4.8) of the diffusion equation, not restricting ourselves to large  $u$ . We pay special attention to the pole structure in the variable  $\omega$ , related to the angular momentum through  $j = \omega - 1$ , and the influence of the boundary conditions. Our approach, which seems natural for the BFKL and the DGLAP equations, is to consider solutions only at  $u \geq u_0$ , when  $u_0$  is not small but also not very far from the infrared region. On the line  $u = u_0$  a boundary condition representing the soft physics must be given. Of course, it is not possible to choose a  $u_0$  where *only* soft physics enter at the boundary; depending on  $u = u_0$  a varying amount of hard physics will already be contained in the boundary condition.

In the variables  $\omega$  and  $u$ , we thus obtain as solution of Eq.(4.7)

$$\bar{h}_1(\omega, u) = \bar{h}_1(\omega, u_0) \frac{\text{Ai}(z)}{\text{Ai}(z_0)} , \quad (4.16)$$

where  $\bar{h}_1(\omega, u_0)$  is the boundary condition. The arguments of the Airy functions  $z = z(\omega, u)$  and  $z_0 = z(\omega, u_0)$  depend on  $\omega$  and  $u$  as given in Eq.(4.8). From the point of view of Regge phenomenology it is obvious to assume that  $\bar{h}_1(\omega, u_0)$  is represented as a sum of Regge poles, some of them having a supercritical intercept,

$$\bar{h}_1(\omega, u_0) = \sum_i \frac{\gamma_i(\omega, u_0)}{\omega - \Delta_i} . \quad (4.17)$$

As said above, in addition to singularities coming from soft physics, some poles contained in the boundary condition, Eq.(4.17), are connected to the hard physics contained in the BFKL diffusion kernel.

Poles in Eq.(4.16) can also arise from zeros of the denominator. These additional poles occur when the argument  $z$  of the Airy function in Eq.(4.8) is negative. This provides an upper bound on the spectrum of the singularities in  $\omega$  arising from the Airy function,

$$\omega_{max} < \frac{\tilde{\Delta}}{u_0} = 4\bar{\alpha}_s(u_0) \log(2) . \quad (4.18)$$

We see that the most right singularity in the complex angular momentum plane,  $j$ , is smaller than the BFKL intercept calculated with the coupling constant at the boundary scale  $u_0$ . The position of the zeros of the Airy function are with high precision given by the formula [17]  $z = -(3\pi n/2 - 3\pi/8)^{2/3}$  with  $n$  a positive integer. We can find an approximate value for  $\omega_{max}$  by inserting  $\omega_{max} = \tilde{\Delta}/u_0 - \epsilon$  into the expression for  $z(\omega, u)$ . Solving for  $\epsilon$ , we find

$$\omega_{max} = \frac{\tilde{\Delta}}{u_0} \left[ 1 - \frac{1}{u_0^{2/3}} \left( \frac{9\pi}{8\kappa} \right)^{2/3} \right] , \quad (4.19)$$

with  $\kappa = (\tilde{\Delta}/\tilde{B})^{1/2} \approx 0.47$ . It is also possible to obtain the locations of the poles in the limit  $\omega \ll \tilde{\Delta}/u_0$  where  $z_0 \simeq -(\kappa\tilde{\Delta}/\omega)^{2/3}$ . The zeros in the denominator then result in poles located at

$$\omega \simeq \omega_n = \tilde{\Delta}\kappa \left[ \frac{3}{2}\pi n - \frac{3}{8}\pi \right]^{-1}. \quad (4.20)$$

This shows that in the diffusion approximation with running coupling constant, the solution contains an infinite set of poles accumulating at  $\omega = 0$  for  $n \rightarrow \infty$ . Such a sequence of poles was already found in the  $\lambda\phi_6^3$ -model in Ref. [18]. In QCD this sequence of poles was first found by Lipatov [5], starting from the same generalization of BFKL to a running gauge coupling, but using different techniques. The discussion of these poles in Ref. [9] is more close to ours.

To clarify the importance of the poles  $\omega_n$ , we calculate their contribution to  $h_1(y, u)$ . Performing the inverse Laplace transformation over  $\omega$  we obtain

$$h_1(y, u) = \sum_i e^{y\Delta_i} \lambda(\Delta_i, u) + \sum_{n=1}^{\infty} e^{y\omega_n} \lambda(\omega_n, u), \quad (4.21)$$

where the first term is the contribution from the (mainly soft) singularities  $\Delta_i$  of Eq.(4.17) and the second that from the Airy function in the denominator;  $\lambda(\eta, u)$  denotes the residue of a pole at  $\omega = \eta$ . The residues of the second term,  $\lambda(\omega_n, u)$ , initially oscillate in  $u$  and can be large up to  $u \sim 3\pi n/2\kappa$ . After that, for  $u \gg u_0$  and large  $n$ , they are proportional to

$$\lambda(\omega_n, u) \sim \text{Ai} \left( \left[ \frac{2}{3\pi n} \right]^{1/3} \kappa u - \left[ \frac{3\pi n}{2} \right]^{2/3} \right) \sim \exp \left( -\frac{1}{\sqrt{\pi n}} \left( \frac{2\kappa u}{3} \right)^{3/2} \right). \quad (4.22)$$

We see that for large  $n$ , where  $\omega_n \rightarrow 0$ , the residues increase and they become “harder”. Because the residues go quickly to zero, only the largest  $n$  values are essential at very high  $u$ . The  $u$  dependence of the residue of a pole at  $\omega_n$  scales with  $\kappa^{-1}n^{1/3}$ . Thus singularities in the sequence  $\omega_n$  more to the right (*i.e.* to larger values) are softer.

For large  $u$ , it is simple to estimate the contribution from large  $n$  to  $h_1(y, u)$ , Eq.(4.21):

$$h_1(y, u) \simeq \sum_n \tilde{\phi}_n(u) \exp \left( -\frac{1}{\sqrt{\pi n}} \left( \frac{2\kappa u}{3} \right)^{3/2} + \frac{2\tilde{\Delta}\kappa}{3\pi n} \right), \quad (4.23)$$

where  $\tilde{\phi}_n(u)$  are weakly dependent on  $u$ . The largest term in this series is at the point  $n = (6\tilde{\Delta}^2/\pi\kappa) y^2/u^3$ . Hence the sum can be estimated as

$$h_1(y, u) \sim \exp \left( y\tilde{\Delta}/u - u^3\tilde{\Delta}/9\tilde{B}y \right), \quad (4.24)$$

which is similar to the solution, Eq.(4.12). So we see that the sum of poles from the BFKL kernel at high  $u$  can be represented by an effective  $u$  dependent intercept with  $\Delta_{\text{eff}}(u) = \tilde{\Delta}/u$ .

We now comment briefly on the connection between the boundary condition,  $h_1(\omega, u_0)$  and the BFKL kernel in Eq.(4.8). As can be seen from Eq.(4.18), choosing a larger starting value  $u_0$  moves the upper limit  $\omega_{\text{max}}$  of the spectrum of poles in  $\omega$  to the left. In order to lead to the same result for  $h_1(\omega, u)$ , independent of  $u_0$ , this change in the kernel due to the poles near  $\omega_{\text{max}}$ , has to be compensated by a concomitant change in the boundary function  $h_1(\omega, u_0)$ . For example, a pole at  $\omega_k$  can be removed by a zero of  $h_1(\omega_k, u_0)$ . If, on the other hand,  $u_0$  is decreased, a pole  $\Delta_i$  originally in the boundary function will move into the BFKL kernel. This connection shows that for a stable choice of  $u_0$ , the boundary has to be in a region where the BFKL equation, and especially the diffusion approximation, is already applicable.

While we have found an infinite set of poles accumulating towards  $\omega = 0$ , for a fixed coupling constant there is a *cut* in the  $\omega$ -plane (see Fig 3.). It was remarked in Ref. [5] that the sequence of poles  $\omega_n$  for running  $\alpha_s$  in some sense corresponds to a cut in the  $\omega$ -plane for fixed  $\alpha_s$ . But this analogue is incomplete as far as we can see for our case with  $t = 0$  (forward scattering). For fixed  $\alpha_s$  the right part of the cut corresponds to the hard Pomeron with mean  $\langle u \rangle \sim \sqrt{y}$ , while for running  $\alpha_s$  the right poles are relatively soft with  $\langle u \rangle \sim 1$ , and only the left side of the sequence  $\omega_n$  towards  $\omega = 0$  becomes hard. These poles may even be artifacts due to our particular choice of running  $\alpha_s$ , which allowed an analytical solution. Furthermore, they may disappear when other higher order corrections to the Pomeron, for example the mixing with multigluon states in the  $t$ -channel, are taken into account. These questions go beyond the scope of our paper and need more investigation.

We can get a slightly different view on the evolution of the gluon ladder and the structure of the  $\omega_n$ -poles by considering a quantum mechanical analogy. Eq.(4.4) can be seen as the Schrödinger equation for a one-dimensional motion in the coordinate  $u$  in the interval  $u_0 < u < \infty$ . The energy of this motion — when time is identified with  $t = -iy$  — is given by

$$E = \frac{1}{2m(u)} \hat{p}^2 + V(u) , \quad (4.25)$$

where we defined the momentum, potential and coordinate dependent mass, respectively, as

$$\hat{p} = -i\hat{\beta} = -i\partial/\partial u , \quad (4.26)$$

$$V(u) = -\tilde{\Delta}/u , \quad (4.27)$$

$$m(u) = u/2\tilde{B} . \quad (4.28)$$

In the case of a constant  $\alpha_s$  we have free motion. So when we put the “particle”, represented by a wave packet, at an initial time at some position  $u_0$ , then the situation at a later time is described by the Green’s function for free motion, Eq.(2.15), yielding propagation and spreading of the wave packet. But for running  $\alpha_s$  the motion is not free; we have a long ranged attractive force in the direction to smaller “distances”  $u$ . In this potential an infinite “Coulomb-like” series of bound states exist. For the high lying states, the particle is located on the average at large distances  $u \gg u_0$  where the motion is quasiclassical. To find their energy spectrum,  $E_n$ , we use the standard quasiclassical quantization condition

$$n\pi = \int_{u_0}^{u_{max}(n)} du p(u) = \int_{u_0}^{\tilde{\Delta}/E_n} du \sqrt{\left[ \frac{\tilde{\Delta} - E_n u}{\tilde{B}} \right]} \simeq \frac{2}{3} \sqrt{\left( \frac{\tilde{\Delta}}{\tilde{B}} \right) \frac{\tilde{\Delta}}{E_n}} , \quad (4.29)$$

which leads to  $E_n = (1/n) \cdot (2\tilde{\Delta}^{3/2}/3\pi\tilde{B}^{1/2})$ , coinciding with Eq.(4.20) in the limit of large  $n$ . It is interesting to note that the behaviour of the residues in Eq.(4.22) corresponds to the motion of our fictitious particle in the classically forbidden region  $u > \tilde{\Delta}/E_n$ . The momenta in this region are not constant due to the  $u$  dependence of the mass,

$$p_n(u) = \sqrt{-2m(u)E_n} = i\sqrt{\frac{2\kappa^3}{3\pi} \frac{u}{n}} . \quad (4.30)$$

Using the wave function  $\lambda_n(u) \sim \exp(iup_n(u))$ , we obtain the same result as in Eq.(4.22).

So far we have excluded the particle from the region  $u < u_0$ , corresponding to an infinite potential barrier. We can change the potential (and thus the boundary condition at  $u_0$ ) in order to allow the “particle” to go to smaller  $u$ . This can for example be achieved if we choose the potential

$$V(u) = -\frac{\tilde{\Delta}}{\log(v(u) + e^u)} , \quad (4.31)$$

where the function  $v(u) \rightarrow 0$  at  $u \rightarrow \infty$  and  $v(u) \rightarrow v_0 > 1$  at  $u \rightarrow -\infty$ . At large  $u > 0$  we have the same potential as before but now we can put  $u_0 = -\infty$ . In this case the motion in  $u < 0$  will be unlimited also for some  $E < 0$ , and all discrete eigenvalues  $E_n$  disappear. In addition, we can choose  $v(u)$  in such a way that  $V(u)$  will have a local minimum at  $u \sim 1$  so that we generate a low lying bound state. In terms of our pole structure in  $\omega$ , this corresponds to a “soft” state with a high intercept resulting from this potential.

In Ref. [19] the structure of the BFKL Pomeron for  $t < 0$  was studied. It is amusing that we can arrive at their findings concerning the Pomeron trajectory by using the following shortcut based on our quantum-mechanical analogue. The position of the Pomeron pole at some momentum transfer  $t < 0$  can be simulated from our  $t = 0$  example by restricting the range of the “coordinate”  $u$  (*i.e.* the range of the transverse momenta, through the condition  $u > u_0 = \log(-t)$ ). We choose in Eq.(4.29) a large  $u_0$  and simply put  $n = 1$  to obtain the leading BFKL Pomeron trajectory,

$$\omega_P(t) \simeq E_1 \simeq \frac{\tilde{\Delta}}{u_0(t)} , \quad (4.32)$$

where  $u_0 = \log(-t/\Lambda^2) \gg 1$ . The trajectories for the other “satellite” poles also can be estimated for large  $u_0$  from Eq.(4.29),

$$\omega_n(u_0) \simeq \Delta(u_0) \left[ 1 - \left( \frac{3\pi}{2\kappa} \frac{n}{u_0} \right)^{2/3} \right] . \quad (4.33)$$

These relations for the Pomeron trajectory coincide with the ones that were found in Ref. [19] in a precise (and therefore more complicated) way. The above results also show the explicit dependence on the infrared cut-off  $u_0$ .

In conclusion, we repeat that the general significance of the poles at  $\omega_n$  needs future investigation. They may be a feature closely connected to our particular choice of the running coupling constant. It will be shown below that for large  $u$  their contribution is small in comparison with the  $\beta \sim 0$  part of the kernel, corresponding to the DGLAP mechanism.

## 5. POMERON WITH HARD ENDS

Eq.(4.1) has the structure of the kinetic equation. The differential equation (4.4) discussed above corresponds to the diffusion approximation, where fast increases in the “coordinate”  $u$  do not occur. For the BFKL Pomeron with fixed  $\alpha_s$  such jumps in  $k_\perp$  are not essential, because the splitting of gluons is universal for all  $k_\perp$  and the diffusion mechanism is sufficient to evolve the gluon distribution in the “time”  $y$  to obtain  $f(y, u)$  at larger  $u$ . All possible inhomogeneities, arising from initial conditions or the infrared region, are smeared out by diffusion.

As we saw above, for the BFKL Pomeron with running  $\alpha_s$  the situation is different. In the diffusion approximation, for which the vicinity around  $\beta = 1/2$  of  $\mathcal{L}$  is essential, the gluon splitting probability  $\tilde{B}\alpha_s(u)$  at large  $k_\perp$  decreases with  $u$ . Therefore only a small fraction of the initially moderate  $k_\perp$  gluons diffuses to the region of larger  $k_\perp$ . As a result the density  $f(y, u) \sim ue^{-u/2}h(y, u)$  decreases fast with  $u$ . This has been discussed in detail above.

In contrast to the diffusion-like behaviour resulting from the expansion of the BFKL kernel  $\tilde{\mathcal{L}}$  around its minimum, the limit  $\beta \rightarrow 0$  of the kernel leads to a growth of  $f(y, u)$  as function of  $u$  as shown in Eq.(3.19). For a BFKL Pomeron with running  $\alpha_s$  only this part can generate a significant contribution at large  $u$ . In this section we briefly show how these previous results, the low  $x$  DGLAP solution, Eq.(3.19), follow quite directly from the BFKL operator equation Eq.(4.1).

It is well known that a DGLAP-like evolution equation follows simply from BFKL when one takes into account only configurations strongly ordered in  $k_\perp$ ; this limiting case corresponds to the part of the eigenvalue spectrum  $\tilde{\mathcal{L}}(\beta)$  situated at  $\beta \rightarrow 0$ , where  $\tilde{\mathcal{L}}(\beta) \sim 1/\beta$ . In the operator equation (4.1), the rapidly increasing part of the BFKL Pomeron is found by using the approximation to the BFKL operator

$$\mathcal{L}(\hat{\beta}) \simeq \hat{\beta}^{-1} = \int^u du' [\dots] . \quad (5.1)$$

Thus instead of Eq.(4.4) we get the integral equation

$$\frac{1}{b\alpha_s(u)} \frac{\partial h_1(y, u)}{\partial y} = \tilde{\alpha}_s \left[ \int_{u_0}^u du' h_1(y, u') + h_1(y, u_0) \right] . \quad (5.2)$$

This approximation is plausible if one looks at Eq.(2.2): take  $k_\perp \gg q_\perp$  in the integral of Eq.(4.1), which then transforms directly into Eq.(5.2) if we introduce the same integration limits. Eq.(5.2) can be solved by means of a Laplace transformation in  $y$  and taking the derivative with respect to  $u$ , which yields

$$h_1(y, u) = \int_{c-i\infty}^{c+i\infty} d\omega e^{\omega y} \bar{h}_1(\omega, u_0) \left( \frac{\alpha_s(u_0)}{\alpha_s(u)} \right)^{-1+\tilde{\alpha}_s/\omega} , \quad (5.3)$$

which is the same DGLAP asymptotic solution as in Eq.(3.15).

From our considerations follows a simple model for the Pomeron suitable for cases when one probes the Pomeron in a hard process, as in deep-inelastic scattering. In fact it is prompted by Eq.(5.3), where  $h_1(y, u)$  is written as the inverse Laplace transformation of the product of two functions: the first function is the boundary condition function  $\bar{h}_1(\omega, u_0)$ , containing mainly the soft, non-perturbative physics, and the second one is the BFKL kernel with running  $\alpha_s$ ,  $\bar{K}_{hard}(\omega, u)$ , containing the essential singularity in  $\omega$ . For the boundary condition we expect a supercritical behaviour and therefore use the function given in Eq.(3.20). We use this structure to directly model the unintegrated gluon distribution  $f(y, u)$ . For our model we choose <sup>2</sup>

$$f(y, u) = f_0 \int_0^y dy_1 e^{(y-y_1)\Delta_0} K_{hard}(y_1, u) , \quad (5.4)$$

where

$$K_{hard}(y, u) = \frac{1}{2\pi i} \int_{c-i\infty}^{c+i\infty} d\omega e^{\omega y} \bar{K}_{hard}(\omega, u) . \quad (5.5)$$

Since we are interested in a hard process where  $u$  is large, we can model  $K_{hard}(y, u)$  by a DGLAP-type kernel that contains all essential features found in Section 3:

$$K_{hard}(y, u) \simeq I_0(2\sqrt{y\xi(u)}) , \quad (5.6)$$

with  $I_0$  the zeroth order modified Bessel function depending on the “invariant charge”

$$\xi(u) \equiv \tilde{\alpha}_s \log \frac{\alpha_s(u_0)}{\alpha_s(u)} . \quad (5.7)$$

---

<sup>2</sup>A similar expression was already proposed in Ref. [22] in the context of the linked dipole chain model [23]. In Ref. [22] it represents an interpolation between DGLAP and the hard BFKL Pomeron. We thank G.Gustafson for his remarks.

In Eq.(5.4), the transverse momenta of the gluons are large up to  $y_1$ . The values of  $y_1$  where the dominant contribution to the integral in Eq.(5.4) comes from, can in general depend on the total rapidity  $y$ . However, since the  $y$  dependence of the integrand factorizes in our model, it is obvious that the dominant  $y_1$  region at very large  $y$  only depends on  $u$ , being independent of  $y$ . We calculate the dominant interval  $y_1$  below.

Expanding the modified Bessel function  $I_0$ , one obtains

$$f(y, u) = f_0 e^{y\Delta_0} \frac{1}{\Delta_0} \sum_{n=0}^{\infty} \frac{1}{n!} \left[ \frac{\gamma(n+1, y\Delta_0)}{n!} \right] \left( \frac{\xi(u)}{\Delta_0} \right)^n , \quad (5.8)$$

where  $\gamma(n, x)$  is the incomplete  $\Gamma$ -function.

For large  $y$ , the Bessel function can be approximated as

$$I_0(2\sqrt{y\xi(u)}) \simeq \frac{1}{2\sqrt{\pi}\sqrt{y\xi}} \exp(2\sqrt{y\xi(u)}) , \quad (5.9)$$

and the integral in our model, Eq.(5.4), can be extended to  $\infty$ . It then can be done analytically [17],

$$f(y, u) = f_0 \int_0^y dy_1 e^{(y-y_1)\Delta_0} I_0(2\sqrt{y_1\xi(u)}) \simeq f_0 e^{\Delta_0 y} \int_0^{\infty} dy_1 e^{-y_1\Delta_0} I_0(2\sqrt{y_1\xi(u)}) \quad (5.10)$$

$$= \frac{f_0}{\Delta_0} e^{\Delta_0 y + \xi(u)/\Delta_0} = \frac{f_0}{\Delta_0} e^{\Delta_0 y} \left( \frac{u}{u_0} \right)^{\frac{3}{\pi b \Delta_0}} . \quad (5.11)$$

This answer can also be obtained from Eq.(5.8) by noting that for  $y \rightarrow \infty$  the factors between brackets approach 1 so that Eq.(5.8) reduces to Eq.(5.11). The solution shows, as expected, a  $y$  dependence characterized by the Pomeron intercept  $\Delta_0$  that originates from the soft boundary, and has multiplicative hard corrections, which again involve  $\Delta_0$ . For large  $y$ , the dominant contribution to the above integral can be easily shown to come from the region around a saddle point at

$$y_1^{(s)} = \xi(u)/\Delta_0^2 . \quad (5.12)$$

The quantity  $\Delta_0 \sim 0.1 - 0.3$  is small, and depends on the chosen boundary condition (*i.e.* on the intercept of the Pomeron at scale  $u_0$ ). The invariant charge  $\xi(u)$  starts to grow relatively fast at  $u_0$  as can be seen from Eq.(5.7). The subsequent growth becomes very slow due to its doubly logarithmic form. For a boundary scale  $k_0^2 = 2 \text{ GeV}^2$  and  $\Lambda = 0.2 \text{ GeV}$ , one obtains  $\xi(u) = 0.3$  at  $k_\perp^2 = 5 \text{ GeV}^2$ ,  $\xi(u) = 1$  at  $k_\perp^2 = 10^2 \text{ GeV}^2$  up to  $\xi(u) = 1.7$  at a very large scale,  $k_\perp^2 = 10^4 \text{ GeV}^2$ . Since the denominator in Eq.(5.12) is small, the saddle point  $y_1^{(s)}$  is already large – of order 10 – at moderate transverse momenta.

A similar estimate for the relevant rapidities  $y_1$  can be obtained by calculating the mean  $y_1$ , weighted with the normalized integrand in Eq.(5.4):

$$\langle y_1 \rangle = (\xi(u) + \Delta_0)/\Delta_0^2 \simeq y_1^{(s)} . \quad (5.13)$$

For the fluctuation around the mean of  $y_1$  one finds

$$\delta y_1 = \sqrt{\langle y_1^2 \rangle - \langle y_1 \rangle^2} = \sqrt{\frac{2\xi(u) + \Delta_0}{\Delta_0^3}} \simeq \sqrt{\frac{2y_1^{(s)}}{\Delta_0}} , \quad (5.14)$$

which shows that the fluctuations in  $y_1$  around its mean are proportional to  $1/\sqrt{y_1^{(s)}}$  and thus small for  $y_1^{(s)} \gg 2/\Delta_0$ .

In current experiments the available maximum rapidity  $y$  is of order 10. For such energies the saddle point  $y_1^{(s)}$  can be large with respect to  $y$  and even exceed  $y$ . As a consequence, it is then not correct to extend the integration range in Eq.(5.10) to infinity. If  $y/y_1^{(s)}$  is small, a more adequate representation of Eq.(5.11) is given by

$$f(y, u) = f_0 \sum_{n=0}^{\infty} \left( \frac{y}{y_1^{(s)}} \right)^{n/2} I_n(2\sqrt{y\xi(u)}) . \quad (5.15)$$

Coming back to Eq.(5.4), we see that our model provides us with a prescription how to incorporate the hard part of the Pomeron,  $K_{hard}(y, u)$ , in reaction amplitudes based on the exchange of Reggeons when  $y$  is large. In this framework it is simple to calculate other quantities. In the amplitude for “onium-onium” scattering with virtualities  $u_1$  and  $u_2$ , the contribution of the Pomeron can be written as

$$A(y, u_1, u_2) \sim \int_0^\infty dy_1 dy_2 dy_3 K_{hard}(y_1, u_1) f_0 e^{\Delta_0 y_2} K_{hard}(y_3, u_2) \delta(y - y_1 - y_2 - y_3) . \quad (5.16)$$

It corresponds to a Pomeron that contains soft physics, in between two hard ends and can be diagrammatically represented by Fig.4. In the language of Regge theory, this contribution is an enhanced diagram. In the limit of  $y \rightarrow \infty$  the ends can be considered as vertices,

$$A(y, u_1, u_2) = g(u_1) f_0 e^{\Delta_0 y} g(u_2) , \quad (5.17)$$

where the hard vertices have the asymptotic form

$$g(u) = g_0 \exp(\xi(u)/\Delta_0) . \quad (5.18)$$

One can apply the hard probe to the Pomeron not only at the ends. When we calculate the inclusive cross section of the production of a hard gluon (jet) with rapidity in the central region, we get a result analogous to Eq.(5.16). If we assume for simplicity that  $y \rightarrow \infty$ , so that the hard parts become hard vertices as in Eq.(5.17), we obtain

$$A_{inel}(y, y_1, u_1, u, u_2) = f_0^2 g(u_1) g(u_2) e^{y\Delta_0} \int_0^{y_1} dy_a \int_0^{y-y_1} dy_b K_{hard}(y_a, u) e^{-\Delta_0(y_a+y_b)} K_{hard}(y_b, u) , \quad (5.19)$$

where  $y_1$  and  $u$  are the rapidity and  $\log(k_\perp^2)$  of the measured gluon(jet), respectively.

Finally, we compare the fixed and running  $\alpha_s$  cases for onium-onium scattering, which is usually considered as a “laboratory” for the perturbative BFKL equation. For simplicity, we choose similar onia with small transverse sizes  $R_\perp^2$ . The transverse momenta of the gluons at the ends of the ladders are then large:  $u_1 = u_2 \sim \log \frac{1}{(R_\perp)^2}$ . The coupling constant at these scales is of order  $1/u_1$ . Because in our example the two onia are equivalent, the internal structure of the Pomeron is symmetric around the middle, where the rapidity is half of the large full interval  $y$ . Therefore we only consider the first half of the ladder. At the beginning of the ladder, for rapidities  $y_1 \ll u_1$ , the simple two gluon exchange model for the Pomeron is in fact adequate, since there is no need for resumming the  $\alpha_s y_1$  contributions, which are small in this region. This holds for both fixed and running coupling constant. After this stage, for a fixed coupling constant one enters into the true BFKL regime. The mean  $u$  of a gluon in the Pomeron ladder at rapidity interval  $y_1$  is first approximately constant and of order  $u_1$ ; due to the diffusion the transverse momenta spread out with rapidity,  $\langle u - \langle u \rangle \rangle^2 \sim y_1$ , but this spreading happens equally towards lower and larger  $u$ . Then at rapidities  $y_1 \sim u_1^2$  the transverse momenta of a substantial amount of gluons can reach small values,  $u \sim 1$ . A boundary condition supplied at low transverse momenta then “prohibits” the transverse momenta

$u$  to diffuse into the soft region. As a consequence, the mean transverse momenta in the ladder start to grow in this region. For running  $\alpha_s$  the situation is different; now the amplitude is given by Eq.(5.17). The transverse momenta, or  $u$ , decrease in large steps, but remain large up to rapidities  $y_1 \sim \xi(u)/\Delta_0^2$ . At this point they reach the soft regime. In the limit of very large  $y$  the ends are relatively small and the soft part covers the most part of the rapidity interval  $y$ .

We thus obtained a model for the Pomeron in hard scatterings that lends itself to a simple diagrammatic interpretation. In this model the Pomeron with a running  $\alpha_s$  is of soft, nonperturbative nature, but it has hard ends when probed in hard scatterings. The hard ends become small in the limit of very large  $y$ . However, in the current deep-inelastic scattering experiments the total rapidity intervals are to small to see the soft nature of the Pomeron since the hard ends are large, thus leading to large hard corrections.

## 6. CONCLUSION

The original derivation of the BFKL Pomeron was carried out for a fixed coupling constant in the leading logarithmic approximation,  $\alpha_s y \sim 1$ . The physical picture behind it is a gluonic ladder where the rungs are strongly ordered in rapidity, the so called multiregge kinematics. Given a characteristic scale at one end of the ladder, the transverse momenta of the gluons diffuse. The variance of  $u = \log(k_\perp^2)$  is of the order of  $y$ , the total rapidity difference along the ladder. The “hard” BFKL Pomeron applies if this diffusion doesn’t reach into the soft nonperturbative regime. The gluon splitting along the ladder leads to the exponential growth of the gluon density with rapidity, characterized by the BFKL intercept  $\Delta \sim 2.6 \alpha_s$ . This intercept follows from a cut in the complex angular momentum plane.

Assuming a standard form for  $\alpha_s(k_\perp)$ , we extended the BFKL equation to the case of a running coupling constant. We were able to obtain an analytical solution for the gluon distribution, transformed to  $\beta$  and  $\omega$ , the conjugate variables of  $u$  and  $y$ . It has an essential singularity at  $\omega = 0$ , corresponding to a cross section of the form  $e^{c\sqrt{y}}$ . As a consequence, the singularities introduced through the boundary conditions at some low scale  $u_0$  are crucial, because they give the dominant contributions if they are to the right of the essential singularity. It was checked that our solution is consistent with the DGLAP expression at large  $y$ , corresponding to low  $x$ .

We expanded our analytical solution for a running coupling constant around  $\beta = 1/2$ . This leads to a diffusion-like equation, where the diffusion and splitting coefficients now depend on  $u$ . This is in contrast to the hard BFKL Pomeron with fixed  $\alpha_s$ , where these coefficients are constant. In this regime the changes in  $u$  along the ladder are relatively small. We found in this approximation an infinite sequence of poles in  $\omega$ , accumulating at  $\omega = 0$ . The poles most to the left are the hardest, *i.e.* most important at large  $u$ . They can be effectively represented by a  $u$  dependent Pomeron intercept, going to 0 for large  $u$ . This behaviour could be explained by considering the semi-classical limit of a quantum mechanical analogue. We also made a simple estimate for the behaviour of the Pomeron trajectory for  $t \neq 0$ .

In general, the diffusion-like part of the solution was found to yield a relatively small contribution if the changes in the transverse momenta are large. The important part is then due to the  $\beta \sim 0$  region of the BFKL operator, where large changes in  $u$  occur. This is similar to the behaviour predicted by the DGLAP equation. We proposed a simple model for large  $u$ , which reflects all the essential properties of the exact solution: a Pomeron which is of nonperturbative origin, but has hard ends when probed by a hard device. In the limit of large  $u$  and large  $y$  a diagrammatic representation was given, which enables one to calculate Pomeron exchange amplitudes quite simply. Onium-onium scattering was discussed as an example in this framework.

In our study we included the running of the coupling constant, an effect we consider the most obvious source of the breaking of scale invariance of the BFKL equation. This led to properties of the resulting Pomeron, which are very different from the characteristics of the perturbative hard Pomeron which one obtains with fixed  $\alpha_s$ . There are of course other higher order corrections which must be taken into account. Examples are corrections to the Lipatov vertices and more complicated multi-gluon exchanges.

Such corrections can still be collected in a modified single Pomeron exchange. There are however also contributions to the reaction amplitude beyond the single Pomeron exchange. They include, for example, the sequential exchange of more than one Pomeron and the “triple Pomeron” interaction. If these multi-Pomeron states become very important, for example at superhigh energies where they are needed to unitarize reaction amplitudes, the significance of the single Pomeron as a building block will be reduced. However, our study has shown that as long as one uses it as a building block, the running of the gauge coupling must be included as it changes the character of the Pomeron significantly.

## ACKNOWLEDGEMENT

We want to thank K.Boreskov and A.Kaidalov for numerous discussions and comments. We are also grateful to V.S.Fadin, V.N.Gribov, G.Gustafson, V.Khoze, Y.A.Simonov, K.A.Ter-Martirosyan for their interest in this work. O.K. would like to thank the theory group of NIKHEF for its hospitality. The work of L.H. and J.K. is part of the research program of the Foundation for Fundamental Research of Matter (FOM) and the National Organization for Scientific Research (NWO). The collaboration between NIKHEF and ITEP was supported by a grant from NWO and by INTAS grant 93-79. O.K. also acknowledges support from grant J74100 of the International Science Foundation and the Russian Government

- [1] V.S.Fadin, E.A.Kuraev, L.N.Lipatov, Sov.Phys.JETP **44** (1976) 443; V.S.Fadin, E.A.Kuraev, L.N.Lipatov, Sov.Phys.JETP **45** (1977) 199; Y.Y.Balitskii and L.N.Lipatov, Sov.J.Nucl.Phys **28** (1978) 822
- [2] F.F.Low, Phys.Rev **D 12** (1975) 163; S.Nussinov, Phys.Rev.Lett. **34** (1975) 1286
- [3] V.S.Fadin and L.N. Lipatov, Preprint DESY 96-020 (1996)
- [4] L.N. Lipatov, Nucl.Phys. **B 365** (1991) 614
- [5] L.N. Lipatov, Sov. Phys. JETP **63** (1986) 904; L.N. Lipatov *in* Perturbative Quantum Chromodynamics Ed. A.H. Mueller, Advanced Series in High Energy Physics (World Scientific Singapore, 1989) 411
- [6] J.Kwiecinski, Z.Phys. **C 29** (1985) 561
- [7] R.E.Hancock and D.A.Ross, Nucl.Phys. **B 383** (1992) 575.
- [8] N.N.Nikolaev and B.G.Zakharov, Phys.Lett **B 327** (1994) 157
- [9] E.M.Levin, TAUP 2221-94, hep-ph 9412345
- [10] M.A.Braun and C.Pajares, Phys. Lett. **B 287** (1992) 154; M.A.Braun and C.Pajares, Nucl.Phys. **B 390** (1993) 542
- [11] G.Camici and M.Ciafoloni, Preprint DFF/260/11/96 (hep-ph/9612235)
- [12] L.P.A. Haakman, O.V. Kancheli, J.H. Koch, Phys.Lett. **B 391** (1997) 157
- [13] O.V. Kancheli, *in* Proceedings of the Workshop “Universality Features in Multihadron Production and the Leading Effect”; Erice, Italy (1996)
- [14] J.C.Collins and P.V.Landshoff, Phys.Lett. **B 276** (1992) 196
- [15] M.F.McDermott, J.R.Forshaw, G.G.Ross, Phys.Lett. **B 349** (1995) 189
- [16] J.Kwiecinski, A.D.Martin, P.J.Sutton Z.Phys. **C 71** (1996) 585
- [17] M. Abramowitz and I.A. Stegun, Handbook of Mathematical Functions
- [18] C.Lovelace Nucl.Phys **B 95** (1975) 12
- [19] R.Kirschner and L.N.Lipatov Z.Phys. **C 45** (1990) 477
- [20] L.V.Gribov, E.M.Levin, M.G.Ryskin, Phys.Rep. **100** (1983) 1; E.M.Levin, M.G.Ryskin, Phys.Rep. **189** (1990) 267
- [21] A.H.Mueller, Nucl.Phys. **B 437** (1995) 107
- [22] B.Andersson, G.Gustafson, J.Samuelsson, Nucl.Phys. **B 467** (1996) 443
- [23] B.Andersson, G.Gustafson, H.Kharraziha, J.Samuelsson, Z.Phys. **C 71** (1996) 613

## FIGURE CAPTIONS

**Fig.1** Contribution of a gluonic ladder with  $n$  rungs to Pomeron exchange. Lipatov vertices are denoted by dots and reggeized gluon propagators by thick vertical gluon lines.

**Fig.2** Solid line:  $\tilde{\mathcal{L}}(\beta)$ . Dashed line:  $\mathcal{R}(\beta)$ .

**Fig.3 a.)** For fixed  $\alpha_s$ : branch cut in the  $\omega$ -plane starting from  $\text{Re } \omega = \Delta$ . **b.)** For running  $\alpha_s$ : series of poles accumulating at  $\omega \rightarrow 0$  starting at  $\text{Re } \omega = \omega_{max}$ .

**Fig.4** Diagrammatic representation of Pomeron exchange in onium-onium scattering. Hatched blocks: hard ends. Middle: soft part of Pomeron.

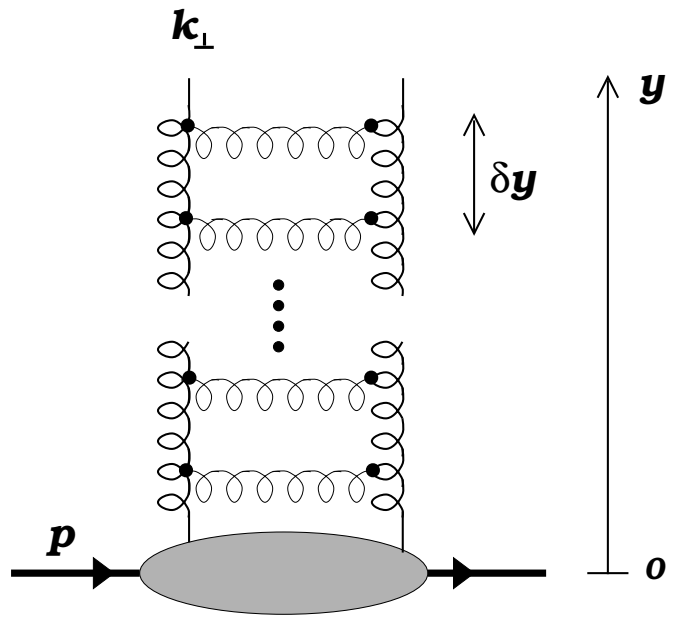


Figure 1

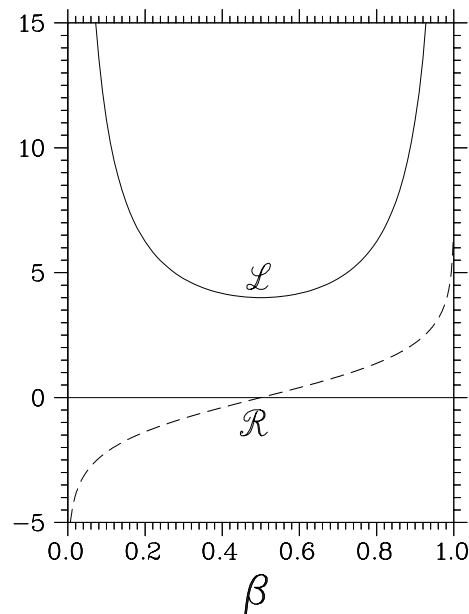
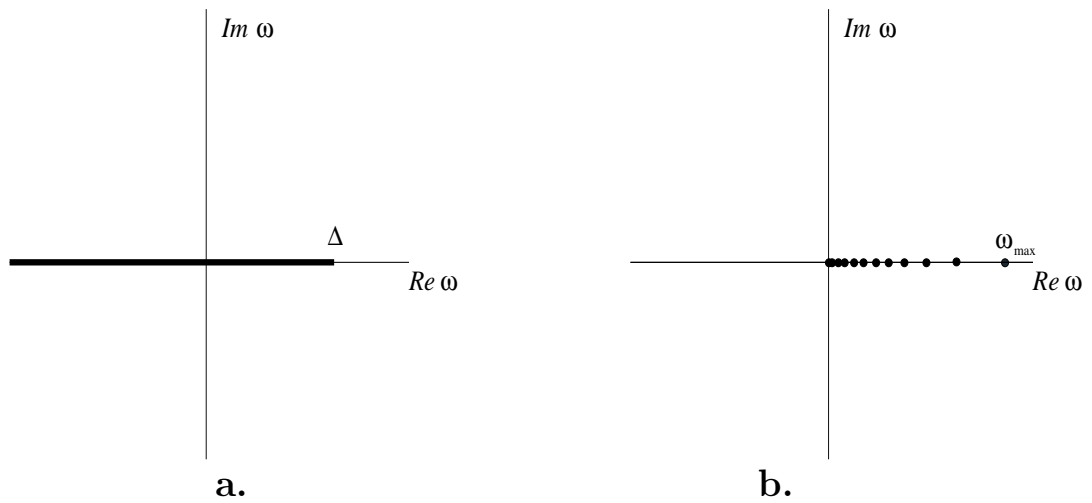
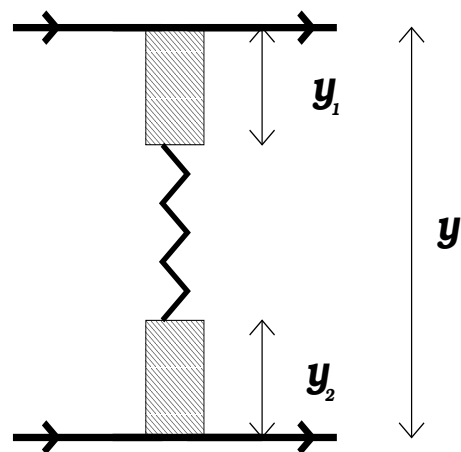


Figure 2



**Figure 3**



**Figure 4**